(3) K. Andres, S. Darack, and S. L. Holt, *Solid State Commun.*, **15**, 1087 (1974).
(4) R. C. Hughes, B. Morosin, P. M. Richards, and W. Duffy, *Phys. Rev. B*, **11**, 1795 (1975).
(5) B. Morosin, *Acta Crystallogr., Sect. B*, **31**, 632 (1975).
(6) Y. Endoh, G. Shirane, R. J. Birgeneau, P. M. Richards, and S. L. Holt, *Phys. Rev. Lett.*, **32**, 170 (1974).
(7) D. Y. Jeter, D. J. Hodgson, and W. E. Hatfield, *Inorg. Chim. Acta*, **5**, 257 (1971).
(8) M. Laing and G. Carr, *J. Chem. Soc. A*, 1141 (1971).
(9) E. Horsfield and M. Laing, *Chem. Commun.*, 735 (1968); E. Horsfield, M. Sc. Thesis, University of Natal, 1968.
(10) K. E. Hyde, B. C. Quinn, and I. P. Yang, *J. Inorg. Nucl. Chem.*, **33**, 2377 (1971).
(11) H. Stieger and W. Ludwig, *Helv. Chim. Acta*, **57**, 2125 (1974).
(12) V. F. Anufrienko, A. P. Terentev, E. G. Rukhadze, and A. G. Onuchina, *Teor. Eksp. Khim.*, **2**, 412 (1966).
(13) J. R. Allan, D. H. Brown, R. H. Nuttall, and D. W. A. Sharp, *J. Chem. Soc. A*, 1031 (1966).
(14) B. K. Mohapatra and D. V. R. Rao, *Indian J. Chem.*, **9**, 715 (1971).
(15) B. K. Mohapatra, *Indian J. Chem.*, **11**, 698 (1973).
(16) V. Gamathy, K. Das, and D. Ghosh, *J. Phys. C*, **8**, 158 (1975).
(17) W. Ludwig and F. Gasser, *Helv. Chim. Acta*, **52**, 2380 (1969).
(18) R. F. Drake and W. E. Hatfield, *Rev. Sci. Instrum.*, **45**, 858 (1974).
(19) Landolt-Börnstein, "Zahlenwerte und Funktionen aus Physik, Chemie, Astronomie, Geophysik und Technik", E. König, Ed., New Series, Group II, Vol. 2, Springer-Verlag, Berlin, 1966.
(20) J. C. Bonner and M. E. Fisher, *Phys. Rev.* [*Sect.*] *A*, **135**, 640 (1964).
(21) R. P. Eckberg and W. E. Hatfield, *J. Chem. Soc., Dalton Trans.*, 616 (1975).
(22) H. P. Stephenson, *J. Chem. Phys.*, **22**, 1077 (1954).
(23) K. T. McGregor, N. T. Watkins, D. L. Lewis, R. F. Drake, D. J. Hodgson, and W. E. Hatfield, *Inorg. Nucl. Chem. Lett.*, **9**, 423 (1973).
(24) H. C. Brown and X. R. Mihm, *J. Am. Chem. Soc.*, **77**, 1723 (1955).
(25) W. Duffy, Jr., and K. P. Barr, *Phys. Rev.*, **165**, 647 (1968).
(26) W. Duffy, J. E. Venneman, D. L. Strandburg, and P. M. Richards, *Phys. Rev. B*, **9**, 2220 (1974).
(27) J. E. Geusic and L. C. Brown, *Phys. Rev.*, **112**, 64 (1956).
(28) K. T. McGregor, R. P. Scaringe, and W. E. Hatfield, *Mol. Phys.*, **30**, 1925 (1975).
(29) H. Abe and K. Ono, *J. Phys. Soc. Jpn.*, **11**, 947 (1956).

Contribution from the Department of Chemistry, The University of British Columbia,
Vancouver, British Columbia, Canada, V6T 1W5

Spectroscopic and Redox Properties of Pseudotetrahedral Copper(II) Complexes. Their Relationship to Copper Proteins

H. YOKOI[1] and A. W. ADDISON*

Received September 20, 1976

AIC60691H

Visible absorption and ESR spectra and redox potentials have been examined for a series of pyrrole-2-carboxaldehyde Schiff base copper(II) complexes, whose coordination stereochemistry is distorted to varying extents from square-planar to pseudotetrahedral geometry. There are smooth correlations among d–d band energies, $A_{\|}$, $g_{\|}$, A_0, and g_0 values. As the dihedral angle between chelate rings increases from 0 through 90°, $g_{\|}$ increases, $|A_{\|}|$ decreases in an antiparallel fashion, and redox potentials shift systematically to more positive values. These observations are consistent with tetrahedral distortion at the metal binding sites of blue copper proteins.

Introduction

There is currently considerable effort being devoted to the elucidation of the composition and geometry of copper binding sites in metalloproteins.[2,5] It has long been recognized that "blue" (type I) copper sites are unusual from the inorganic chemist's viewpoint: they exhibit markedly positive Cu(II)/Cu(I) redox potentials and unique visible absorption and ESR spectra, the latter with extremely small hyperfine interactions.[6] Recently the former two properties have been studied,[7-9] Patterson and Holm having related the unusual redox properties of blue copper proteins to the electrochemical properties of selected low molecular weight copper(II) chelates.[10] Tetrahedral geometry[9,11] and the presence of sulfur donor atoms[7,8,12] have both been proposed for the blue copper sites. Quantitative conclusions with regard to the effect of stereochemistry (particularly tetrahedral distortion) on the redox potential are still in their infancy. Moreover, the paucity of redox and spectroscopic data relating to mononuclear CuN_3S and CuN_2S_2 species with nonconjugated thiolate ligands, coupled with the synthetic intractability of such systems, renders it gainful to deduce parallels between these ligand systems and CuN_4 or CuN_2O_2 centers.

Precise estimation of the degree of tetrahedral distortion of copper(II) complexes in solution is not facile, although several papers on ESR and optical absorption studies have been published,[13-16] including an application to a metal-substituted protein.[17] However, there have been a number of theoretical studies of tetrahedrally coordinated copper(II) centers and correlation with the extensive experimental studies on solid-state systems.[18-25] ESR expressions have thus been derived[21] and applied to interpretation of the spectroscopic parameters of the tetrachlorocuprate(II) ion.

Redox potentials of Cu(II)/Cu(I) systems are related to the relative thermodynamic stabilities of the two oxidation states in a given ligand environment. The factors influencing the metal-localized redox properties of copper systems have been extensively investigated by James and Williams[26] and others.[10,27]

Bis(*N*-substituted-pyrrole-2-carboxaldiminato)copper(II) complexes are of the Schiff base type yet share the pyrrole structural feature with porphyrins. They vary in stereochemistry according to the imino-N substituent, the degree of tetrahedral distortion being defined by the angle ω, as in Figure 1. Diamines yield the tetradentate species, shown as Cu(P2A$_2$-B).

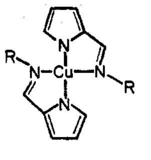

Cu(P2A-R)$_2$

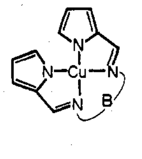

Cu(P2A$_2$-B)

The first aim of this paper is to investigate the ESR and visible absorption spectra of a series of the Cu(P2A-R)$_2$ complexes with various R groups. The second is to survey the electronic features of tetrahedral distortion from the data, together with data so far known for other tetrahedrally dis-

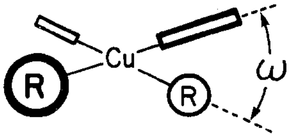

Figure 1. Definition of ω, the angle between chelate ring planes.

Table I. ESR Data for Cu(P2A-R)$_2$ and Cu(P2A$_2$-B) in Toluene

	Obsd[b]				Est[c]	
R or B	$g_\parallel$	$-10^4 A_\parallel$, cm^{-1}	g_0	$-10^4 A_0$, cm^{-1}	$g_\perp$	$-10^4 A_\perp$, cm^{-1}
H[a]	2.182	192	2.093	71	2.049	11
Me	2.197	181	2.192	65	2.055	7
Et	2.199	179	2.103	61	2.055	2
Tfe	2.213	164	2.110	53	2.059	−3
^{n}Pr	2.202	174	2.103	60	2.053	3
^{i}Pr	2.205	171	2.108	54	2.060	−5
^{n}Bu	2.203	175	2.104	60	2.055	−3
^{i}Bu	2.203	173	2.105	58	2.056	1
^{s}Bu	2.212	160	2.108	51	2.056	−4
^{c}Hx	2.205	174	2.107	55	2.058	−5
Norb	2.206	168	2.109	54	2.060	−3
Dpm	2.207	168	2.109	53	2.060	−5
Dma	2.186	188	2.097	68	2.053	−8
^{t}Bu	2.267	108	2.134	14	2.068	−33
Adam	2.265	107	2.133	16	2.067	−30
Dmpe	2.266	105	2.135	12	2.070	−35
en	2.171	210	2.085	81	2.042	17
prn	2.177	207	2.089	80	2.045	17
bun	2.187	194	2.096	73	2.051	13

[a] Abbreviations: Tfe = 2,2,2-trifluoroethyl, ^{c}Hx = cyclohexyl, Norb = *exo*-2-norbornyl, Dpm = diphenylmethyl, Dma = 2′,6′-dimethylphenyl, Adam = 1-adamantyl, Dmpe = α,α-dimethylphenethyl, en = -CH$_2$CH$_2$-, prn = -CH$_2$CH$_2$CH$_2$-, bun = -CH$_2$CH$_2$CH$_2$CH$_2$-, while the other abbreviations have their usual meanings. [b] $g_\parallel \pm 0.002$; $A_\parallel \pm 0.002$ cm^{-1}. [c] $g_\perp$ and $A_\perp$ were calculated from the equations $g_0 = (g_\parallel + 2g_\perp)/3$ and $A_0 = (A_\parallel + 2A_\perp)/3$ using the observed values (left columns) of A_0 and g_0 at 300 K and of $A_\parallel$ and $g_\parallel$ at 77 K.

torted copper(II) complexes, and relate these results to those for copper porphyrins. The third is to investigate the relationship between redox potentials and the degree of tetrahedral distortion using the Cu(P2A-R)$_2$ complexes. The fourth is to comment on "blue" copper sites in metalloproteins on the basis of the results obtained.

Experimental Section

Preparation of Compounds. Reagent grade pyrrole-2-carboxaldehyde and amines were used as supplied by Aldrich Chemical or Eastman Kodak. All the pyrrole-2-carboxaldiminecopper chelates prepared are listed in Table I. Table II contains analytical results for new chelates and those synthesized with some difficulty. The others, which have been well characterised previously,[28-30] were used for physical measurements after recrystallization. Bis(*N*-alkylsalicylaldiminato)copper(II) compounds were synthesized as in the literature,[31,32] as were Ni(P2A$_2$-prn)[33] and Zn(P2A-^{t}Bu)$_2$.[29]

The pyrrole-2-carboxaldimine chelates (except R = H, ^{s}Bu) were prepared by allowing copper(II) acetate hydrate (0.10 mol) to react with pyrrole-2-carboxaldehyde (0.21 mol) and the appropriate amine (0.3 mol) in the presence of redistilled triethylamine (10 mL) in warm 50% ethanol (40 mL). For R = H and ^{s}Bu, pyrrole-2-carboxaldehyde (0.20 mol) and sodium hydroxide (0.20 mol) were dissolved with stirring in 50% ethanol, and copper(II) sulfate pentahydrate (0.10 mol) was added. The product was immediately precipitated by the addition of excess concentrated aqueous ammonia (R = H) or *sec*-butylamine (R = ^{s}Bu) to the solution. Products were purified by recrystallization from ethanol (R = Me, Et, Pr, Bu, Tfe, prn, bun, Dma, Dmpe), acetonitrile (R = Adam, Norb), cyclohexane (R = ^{c}Hx), benzene/hexane (R = Dpm), or dichloromethane (R = H) and dried in vacuo over phosphorus(V) oxide. Yields were 50–90%, except for R = Tfe (35%) and R = Dmpe (10%).

Physical Measurements. Electronic spectra at room temperature in toluene solution were recorded on a Cary-14 spectrophotometer. A solid-state spectrum for Cu(P2A-^{t}Bu)$_2$ was measured from 350 to 800 nm on the same instrument via the so-called opal-glass method[34] using a silicone mull of a finely powdered sample. Toluene was purified by successive shaking with sulfuric acid and sodium hydroxide, followed by drying over sodium and finally fractional distillation.

Table II. Analytical Data for Cu(P2A-R)$_2$ and Cu(P2A$_2$-B)

	% calcd			% found			
R or B[a]	C	H	N	C	H	N	Mp, °C
H	48.1	4.0	22.4	48.2	4.2	22.5	130 dec[b]
Tfe	40.6	2.9	13.5	40.6	2.9	13.6	163
^{i}Bu	59.7	7.2	15.5	59.6	7.4	15.3	199
^{s}Bu	59.7	7.2	15.5	59.6	7.2	15.5	93
^{c}Hx	63.8	7.3	13.5	63.8	7.5	13.3	179
Norb	65.8	6.9	12.8	65.5	7.0	12.6	145–146
Dmp	74.3	5.2	9.6	74.0	5.2	7.4	199–200
Dma	68.2	5.7	12.2	67.9	5.7	12.2	197
Adam	69.5	7.4	10.8	69.6	7.5	10.6	202–203
Dmpe	70.1	6.6	10.9	70.1	6.8	10.8	149–150
bun	55.3	5.3	18.4	55.2	5.4	18.6	151

[a] Abbreviations used are explained in footnote *a* of Table I. [b] Literature[28] dec pt 140 °C.

ESR spectra at room temperature and at −196 °C were recorded on a Varian E-3 X-band spectrometer, the magnetic field strength being calibrated with an NMR probe and with Mn(II) in MgO powder.

A 0.94 mol % solution of Cu(P2A-^{t}Bu)$_2$ in molten Zn(P2A-^{t}Bu)$_2$ was allowed to freeze, and the ESR spectrum of a powdered sample of this at −196 °C was taken as the spectrum of the Cu(II) complex magnetically diluted, as an impurity in the Zn(II) complex lattice.

Mass spectrometry was performed on a Varian MAT CH4-B instrument, operating at 70 eV. Probe temperatures below the melting points of the compounds gave adequate sample volatilization.

Parent ion peaks were the most intense observed for all compounds. Many of the Cu(P2A-R)$_2$ molecules yielded (up to 30% of the total copper) Cu$_2$(P2A-R)$_2^+$ as well.

Cyclic voltammetry (0.3–0.4-mm radius hanging mercury drop electrode) was performed at 25 ± 0.2 °C in acetonitrile which had been refluxed over and then distilled off phosphorus(V) oxide under nitrogen. Solutions deoxygenated by bubbling nitrogen or argon contained as supporting electrolyte 0.1–0.2 M TEAP (tetraethylammonium perchlorate, G. F. Smith polarographic grade, recrystallized from water and dried in vacuo over phosphorus(V) oxide). The electrochemical apparatus used utilizes a PAR-173 potentiostat and PAR-176 i/E converter. Voltammetric data were recorded on a storage oscilloscope or X-Y/X-t chart recorder. The three-electrode cell comprised as the reference a Ag(s)/AgClO$_4$ (0.01 M), TEAP (0.1 M), CH$_3$CN electrode, to which all potentials are referred. We have measured this to be 0.30 V positive of the SCE at 25 °C. C, H, and N analyses were performed at the University of British Columbia by Mr. P. Borda.

Results

ESR Spectra. Representative ESR spectra obtained at −196 °C and at room temperature are shown by Figure 2 to be axial or nearly axial at low temperature.[36] From these low-temperature spectra, the parallel components of the spin-Hamiltonian parameters, $g_\parallel$ ($=g_z$) and $A_\parallel$ ($=A_z$), can be determined with a precision adequate for our purposes. However, exact analysis of the high-field part of the spectra is not easy, especially in cases where the perpendicular components, g_x and g_y or A_x and A_y, are different.[4,34,37] The average values, g_0 and A_0 usually suffice for any discussion of chemical bonding.[38] The average values which can be determined from solution ESR spectra for copper(II) complex molecules in free tumbling motion enable estimation of $g_\perp$ and $A_\perp$ via the relationships $g_0 = (g_\parallel + 2g_\perp)/3$ and $A_0 = (A_\parallel + 2A_\perp)/3$. As toluene is a noncoordinating solvent, dg_0/dT may be presumed negligible[39] over the range 77–300 K. A possible small temperature dependence of A_0 renders approximate the values of $A_\perp$ derived from the room-temperature A_0 values. Most room-temperature ESR spectra obtained consisted of four ill-resolved resonance lines. They were analyzed by a sim-

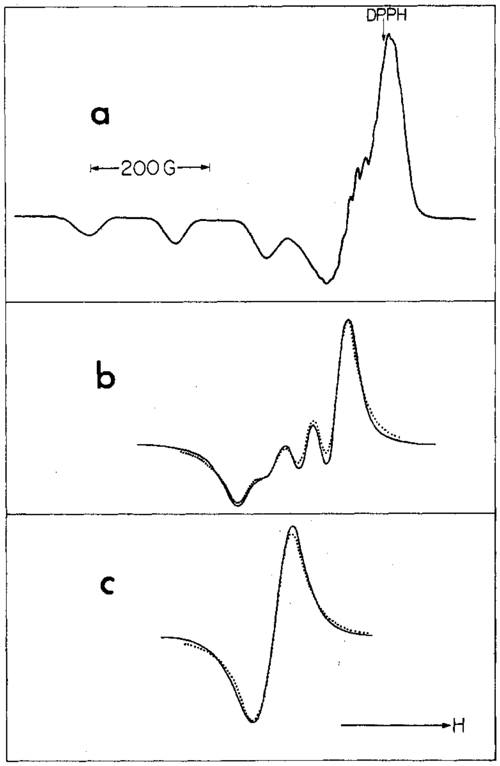

Figure 2. Representative X-band ESR spectra of $Cu(P2A\text{-}R)_2$ in toluene: (a) for R = Norb at 77 K; (b) for R = Norb at ambient temperature; (c) for R = ^{t}Bu at ambient temperature. Dashed lines are spectra simulated with (b) 36, 40, 46, and 55 G and (c) 40, 45, 50, and 55 G for the ΔH's of $M = {}^3/_2, {}^1/_2, -{}^1/_2$, and $-{}^3/_2$ lines, respectively.

ulation method[40] with a second-order (hyperfine-related) correction in the resonance fields.[39] Lorentzian line shapes with four different line widths were used throughout for spectral simulations, and isotope effects due to the natural occurrence of ^{63}Cu and ^{65}Cu were taken into consideration. An example of the spectral simulations is shown in dotted lines in Figure 2.

Solution ESR spectra of the chelates with R = ^{t}Bu, Adam, and Dmpe showed single broad lines, which are quite different in line shape from the others. The same type of spectrum has been observed by Herring et al.[16] for a highly tetrahedrally distorted complex, $[CuMe_2Ga(Dmpz)_2]$, in petroleum, and the onset of an Orbach process was invoked in relationship to the line width. In the $Cu(P2A\text{-}R)_2$ cases, spectra of different line shape could be analyzed simply by allowing for variation in A_0 between species, the analyses yielding internally consistent results, represented by Figures 4 and 7. The ESR results obtained are in Table I.

Visible Absorption Spectra. The visible absorption spectra of the $Cu(P2A\text{-}R)_2$ and $Cu(P2A_2\text{-}B)$ complexes are less obscured by intense bands at shorter wavelength than are those of the salicylaldimine Schiff base complexes. Representative absorption spectra are shown in Figure 3. In the region 10 000–20 000 cm^{-1}, most spectra had an absorption peak (ϵ <300) with a shoulder on the low-energy side. The absorption envelope could be cleanly resolved into just two Gaussian components, this analysis being one which has been applied previously to CuO_4 chromophores, by Graddon[42] and Belford.[43] The results, exemplified by Figure 3, are in Table III.

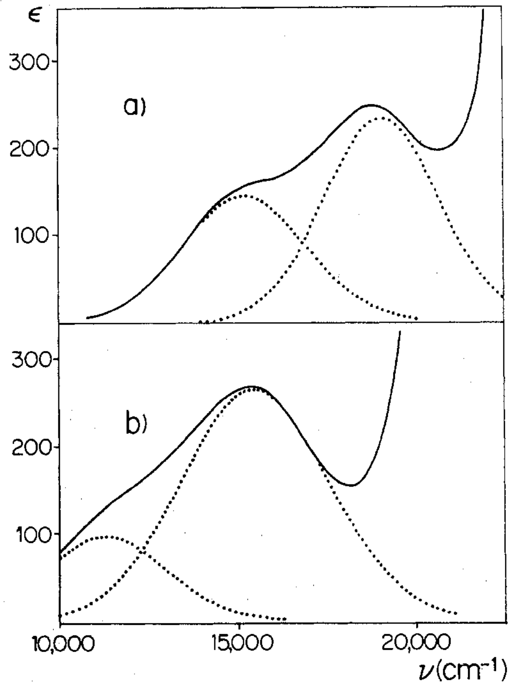

Figure 3. Visible absorption spectra of (a) $Cu(P2A\text{-}Et)_2$ and (b) $Cu(P2A\text{-}Adam)_2$ in toluene. Dashed curve represents Gaussian resolution (see text).

Table III. Visible Absorption Data for $Cu(P2A\text{-}R)_2$ and $Cu(P2A_2\text{-}B)$ in Toluene

R or B	ν_{max}, cm^{-1} (ϵ)	Band I, cm^{-1} (f)[b]	Band II, cm^{-1} (f)
H	(115)[a]	18 000	20 500 sh[c]
Me	19 250 (217)	15 650 (0.002 00)	19 450 (0.003 43)
Et	18 850 (246)	15 250 (0.002 51)	19 150 (0.003 81)
Tfe	18 500 (237)	14 700 (0.002 18)	18 700 (0.004 02)
^{n}Pr	18 800 (251)	15 000 (0.002 23)	18 950 (0.004 25)
^{i}Pr	18 150 (340)	14 500 (0.002 43)	18 450 (0.004 47)
^{n}Bu	18 750 (253)	15 000 (0.002 36)	18 950 (0.004 22)
^{i}Bu	18 750 (266)	14 950 (0.002 62)	18 950 (0.004 41)
^{s}Bu	17 150 (242)	14 150 (0.002 55)	18 100 (0.004 55)
^{c}Hx	18 450 (243)	14 800 (0.002 67)	18 700 (0.004 15)
Norb	18 300 (270)	14 650 (0.003 08)	18 550 (0.004 44)
Dpm	18 000 (243)	14 350 (0.002 54)	18 250 (0.004 23)
Dma	(213)[a]	16 000	20 000 sh
^{t}Bu	15 350 (264)	11 400 (0.001 55)	15 450 (0.005 42)
Adam	15 400 (267)	11 300 (0.001 66)	15 500 (0.005 54)
Dmpe	15 250 (264)	11 450 (0.001 99)	15 300 (0.004 90)
en	18 500 (290)	18 550 (0.000 52)	21 000 sh
prn	17 800 (114)	18 000	21 000 sh
bun	19 900 (158)	16 100 (0.001 28)	19 900 (0.002 66)

[a] Intensity at 18 000 cm^{-1}. [b] Oscillator strength. [c] Shoulder.

Redox Properties. Table IV gives the electrochemical data obtained at the HMDE in acetonitrile, usually at sweep rates of 100 mV s^{-1}, and 0.5–2 mM in Cu. For some of the chelates, non-Faradaic (adsorption) processes were minimized by using higher concentrations (2–7 mM) and lower sweep rate (16.7 mV s^{-1}).[44] The anodic:cathodic current ratios tabulated are at v = 100 mV s^{-1}. All those significantly less than unity increase as the scan rate is increased, with the exception of $Cu(P2A\text{-}H)_2$ and $Cu(P2A_2\text{-}prn)$. The iR-corrected anodic peak to cathodic peak potential separations for the other compounds listed fall in the range (60–75 mV) expected for Nernstian one-electron reduction processes at a spherical microelectrode at the appropriate scan rate.[45] Measurements made in the absence of iR correction yielded values quite comparable to those (65–80 mV) observed for well-established one-electron redox systems. The peak cathodic current function values, corrected for electrode sphericality[45] and essentially independent of scan rate, are as expected for n = 1, $D = 10^{-5}$ cm^2 s^{-1}. The redox processes observed at similar potentials in DMF for $Cu(P2A\text{-}Me)_2$ and $Cu(P2A\text{-}{}^tBu)_2$ have been demonstrated previously to be reversible one-electron processes, and the formation of copper(I) species was thereby

Table IV. Electrochemical Data for $Cu(P2A\text{-}R)_2$ and $Cu(P2A_2\text{-}B)$

Substituent	$-E_{1/2}$,[a] V	$i_{p,a}/i_{p,c}$[b]	$i_{p,c}/cv^{1/2}$,[b,c] mA $s^{1/2}$ M^{-1} $V^{1/2}$
H	1.03[d]	0.70	22.2
Me	0.99	0.95	22.3
Et	0.97	0.94	19.8
Tfe	0.71	1.00	18.5
^{n}Pr	0.99	0.98	19.2
^{i}Pr	0.90	0.98	16.1
^{n}Bu	0.98	0.97	19.3
^{i}Bu	0.97	0.86	20.2
^{s}Bu	0.88	0.99	17.7
^{c}Hx	0.90	0.98	31.3
Norb	0.84	1.00	16.7
Dpm	0.74	0.99	10.0
Dma	0.87[e]	0.88	15.1
^{t}Bu	0.85	0.99	19.3
Adam	0.86	0.93	19.3
Dmpe	0.80	1.0	15.9
en	1.12[f]	1.00	16.6
prn	1.31	0.8	26.4
bun	1.15	0.91	22.2

[a] ±10 mV, vs. $Ag(s)/Ag^+$ (0.01 M), TEAP (0.1 M), CH_3CN reference electrode. [b] ±5%. [c] At HMDE of area 0.022 cm^2. [d] $\frac{1}{2}(E_{p,c} + E_{p,a})$; $E_{p,a} - E_{p,c}$ = 115 mV at 1 V s^{-1} without *iR* correction. [e] Reduction wave observed at $E_{p,c} = -1.10$ V. [f] $E_{p,c}$ + 0.03 V at v = 0.1 V s^{-1}; $E_{p,a} - E_{p,c}$ = 310 mV, in 0.2 M tetrabutylammonium perchlorate.

confirmed coulometrically.[10] On these bases, we accordingly assign the reversible redox processes observed for the $Cu(P2A\text{-}R)_2$ species to the $Cu(II) + e^- \rightleftharpoons Cu(I)$ step. That $Ni(P2A_2\text{-}prn)$ is not reduced until −2.1 V ($E_{p,c}$) also lends credence to the above assignment. The reductions of $Cu(P2A\text{-}H)_2$, $Cu(P2A_2\text{-}en)$, and $Cu(P2A_2\text{-}prn)$ are not thermodynamically reversible under the above experimental conditions. Reduction processes were observable for a number of bis(*N*-alkylsalicylaldiminato)copper(II) molecules, but in acetonitrile, their electrochemistry was often obscured by non-diffusion-controlled processes, and peak potential separations were usually larger (90–150 mV) than expected for reversible reductions. Mean $(-\frac{1}{2}E_{p,c} - \frac{1}{2}E_{p,a})$ peak potentials obtained were as follows (alkyl group, potential (V)): Et, 1.22; ^{i}Pr, 1.10; ^{n}Bu, 1.25; ^{i}Bu, 1.24; ^{s}Bu, 1.09; ^{t}Bu, 1.05; ^{c}Hx, 1.09. Reasonable chemical reversibility ($i_a/i_c > 0.9$) was observed (v = 1–4 V s^{-1}) only for ^{t}Bu, ^{i}Pr, ^{c}Hx, and ^{s}Bu; $i_{p,c}/cv^{1/2}$ values ranged from 21 to 25 mA $s^{1/2}$ M^{-1} $V^{-1/2}$.

Inasmuch as the redox potentials are somewhat solvent dependent,[45] it is important that it be pointed out here that the absorption spectra of the copper pyrrole-2-carboxaldiminates are relatively insensitive to solvent, which is reasonable for a CuN_4 system,[47] as shown by the λ_{max} (ϵ) values for $Cu(P2A\text{-}Me)_2$ in the following solvents: toluene, 520 nm (217); acetonitrile, 501 nm (207); DMF, 503 nm (179), compared to a strongly coordinating solvent, pyridine, 650 nm (100). In addition, there are no significant differences between the ESR spectra in toluene and in toluene/acetonitrile. We therefore consider it justifiable to refer to *parallels* between $E_{1/2}$ changes in acetonitrile vs. other properties in toluene, in our discussion.

Discussion

ESR Parameters. In the crystalline state, $Cu(P2A\text{-}H)_2$ is essentially planar,[48] while $Cu(P2A\text{-}^{t}Bu)_2$ has a pseudotetrahedral coordination geometry with a dihedral angle of about 60° between each of the two coordination planes defined by a CuN_2 moiety.[49] The degree of distortion may be expected to increase as the substituent becomes more bulky, and the same type of distortion must occur in solutions, unless *strongly* coordinating solvent molecules occupy an axial position.

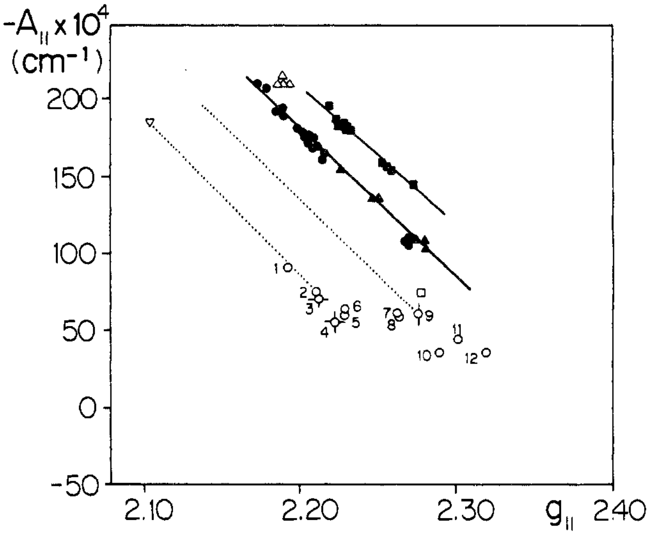

Figure 4. Relationships between $A_{\parallel}$ and $g_{\parallel}$ for copper(II) complexes with (●) pyrrole-2-carboxaldimines, (▲) dipyrromethenes,[14] (△) tetraphenylporphyrins,[50] and (■) salicylaldimines.[15] The points ○ are for selected copper proteins:[6] 1, *P. versicolor* laccase; 2, human ceruloplasmin; 3, *R. succedanea* laccase; 4, *C. sativus* ascorbate oxidase; 5, zucchini ascorbate oxidase; 6, spinach plastocyanin; 7, *P. denitrificans* azurin; 8, *P. fluorescens* azurin; 9, *B. pertusis* azurin; 10, *R. vernicifera* stellacyanin; 11, *R. vernicifera* laccase; 12, horseradish umecyanin. The point ▽ is for a CuN_2S_2 species (see text); □ is for $Cu(P2A\text{-}^{t}Bu)_2$ doped into the Zn(II) lattice.

The tendency for $g_{\parallel}$ to increase and $|A_{\parallel}|$ to decrease with an increase in the degree of tetrahedral distortion has been reported previously for structurally well-characterized complexes of copper(II) with *N*-alkylsalicylaldiminates,[15,17] bis(pyrazolyl)gallates,[16] and dipyrromethenates ($g_{\parallel}$).[14] This tendency is clearly shown in Table II. In addition, a closer inspection of the table indicates that g_0 and A_0 similarly change in an antiparallel fashion, and, furthermore, there is a good linear relationship between $g_{\parallel}$ and $A_{\parallel}$, as demonstrated in Figure 4. By necessity, $g_{\perp}$ and $A_{\perp}$ also increase with $g_{\parallel}$, because they were derived from the above parameters. These facts suggest that $A_{\parallel}$ or $g_{\parallel}$ may be used as an index to the electronic properties of this series of chelates.

Correlation between $g_{\parallel}$ and $A_{\parallel}$ similar to that described above has been observed for the case where coordinate bonding in planar copper(II) complexes is affected by the electron-donating ability of ligands[51] or by apical coordination of basic solvent molecules.[52,53] The latter was obviated via use of toluene solvent for spectroscopic measurements. The effect of increased electron-donating ability (associated with $-CF_3$, $-CH_3$, and $-C(CH_3)_3$ substituents) on the ESR parameters of β-diketonate complexes of copper(II) is to decrease $g_{\parallel}$ and increase $|A_{\parallel}|$.[51] Regardless of whether these changes may be associated with changes in the degree of covalency of the Cu–N interaction, it is clear that the effect of the imino substituent on the ESR parameters is directly opposed to that expected if an inductive effect were dominant, as is evident from Table II. We conclude that a stereochemical factor, namely, the tetrahedral distortion, indeed dominates the trend of $A_{\parallel}$ and $g_{\parallel}$ values in Figure 4.

It is noteworthy that the $|A_0|$ value is reduced by tetrahedral distortion, as shown in Table II. Since the absolute sign of $A_{\parallel}$ in ordinary copper(II) complexes is predicted to be negative on theoretical grounds,[54] it is inferred that $A_{\perp}$ becomes positively large when $|A_0|$ is small. Figure 4 shows the plots of $A_{\parallel}$ against $g_{\parallel}$ comprising most of the ESR data on tetrahedrally distorted copper(II) complexes known to date. All of the $Cu(P2A\text{-}R)_2$ and $Cu(P2A_2\text{-}B)$ chelates are in a straight line, as has been mentioned above. It was a surprise to us that

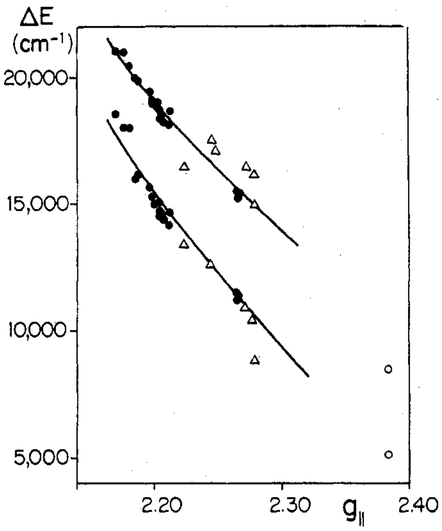

Figure 5. Relationships between d–d transition energies and $g_{\parallel}$, for (●) pyrrole-2-carboxaldimine and (△) dipyrromethene[13] complexes. The points ○ are for $CuCl_4^{2-}$.

so many chelates with the CuN_4 chromophore are on this line, regardless of their degree of tetrahedral distortion and of the chemical diversity of their ligands.

Tetrahedrally distorted bis(dipyrromethenate) and some planar porphyrin complexes fall into the correlation. This suggests, not unreasonably, similarity in coordination environment among these three types of compounds and provides a new perspective toward the elucidation of metal porphyrin electronic structure. Also interesting is the fact that $CuCl_4^{2-}$ in Cs_2CuCl_4 crystals, where the dihedral angle between two coordination planes is known[55] to be about 74°, is near the extension of this line. Despite the different nature of N and Cl donor atoms (except within the framework of HSAB theory, which indeed assigns them similar softness parameters),[55] this observation is likely more than just coincidence. In any case, the interpretation of data for $CuCl_4^{2-}$, which has been examined extensively, both experimentally and theoretically, is prerequisite enough to our understanding of the CuN_4 systems, to warrant further comment (vide infra).

Visible Absorption Spectra. Red shift and intensity enchancement of d–d bands are recognized indicators of the transformation from square-planar to tetrahedral stereochemistry, as exemplified by the results for *N*-alkylsalicylaldiminate complexes of Cu(II)[57] and the pyrrole-2-carboxaldiminate complexes of Ni(II) and Co(II) as well.[29] These properties would reasonably be expected to change in a continuous and parallel fashion, as do the magnetic parameters, as the structures undergo this stereochemical change.[58,59] The Gaussian resolution data for the Cu(P2A-R)$_2$ and Cu(P2A$_2$-B) compounds and the related band energies observed for $CuCl_4^{2-}$ and substituted dipyrromethenate complexes are plotted against $g_{\parallel}$ in Figure 5. The result is two smooth curves, which roughly parallel each other, there being no indication that the two curves intersect in the range of $g_{\parallel}$ shown in the figure. The abscissa in the figure covers possible configurations from square-planar toward tetrahedral geometry, as $\omega = 0°$ for Cu(P2A-H)$_2$ ($g_{\parallel} = 2.182$) and $\omega = 74°$ for $CuCl_4^{2-}$ in crystals[54] ($g_{\parallel} = 2.384$). This figure is the first experimental data set which clearly indicates how d–d band energies change smoothly and continuously with changes in stereochemistry from square-planar toward tetrahedral geometry. According to Ferguson's[19] generally accepted assignment for the ligand field spectrum of $CuCl_4^{2-}$, the relative energies of the d orbitals are $d_{xy} > d_{xz,yz} > d_{x^2-y^2} > d_{z^2}$. In Figure 4, therefore, the lower energy bands can be assigned to both of the d–d transitions d_{xz}, $d_{yz} \rightarrow d_{xy}$, and the higher energy bands, to both of the transitions $d_{x^2-y^2} \rightarrow d_{xy}$ and $d_{z^2} \rightarrow d_{xy}$ (the coordinate system being chosen so that d_{xy} is the ground state, as will be described later). The results shown in Figure 5, however, are contrary to the usual theoretical interpretation by Lohr and Lipscomb,[18] by Smith,[20] and by others,[24,59] with regard to whether or not the energy levels of d_{xz} and d_{yz} intersect those of d_{z^2} or of both d_{z^2} and $d_{x^2-y^2}$ in the range of ω from 0 to 90°; accordingly, our assignments of d–d bands for planar copper(II) complexes do not always agree with many of the assignments so far carried out. One reason for this is probably that there may be some peculiarities resulting from conjugation of the four nitrogen atoms with the large π-electron system. Our assignment is reasonably supported by ESR, as detailed below.

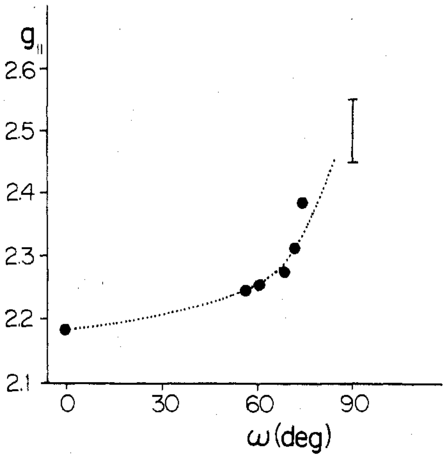

Figure 6. Estimated relationship between $g_{\parallel}$ and ω, from interpolation of calculated 90° limit and data from ref 22, 24, 53, and 57 and this work.

The visible absorption spectrum of Cu(P2A-^{t}Bu)$_2$ in the powder state shows a peak at 15 900 cm^{-1}. This complex in the crystalline state is known to have $\omega = 60°$. Since the absorption peak in the visible region approximately agrees with the higher energy band in position, as shown in Figure 2, the $g_{\parallel}$ value of the complex with $\omega = 60°$ is estimated to be about 2.254 from Figure 4. In toluene solution, this complex has $g_{\parallel} = 2.267$ and a peak energy of 15 350 cm^{-1}. These results indicate that the tetrahedral distortion is a little larger in the solid state than in solution, suggesting that there is some intermolecular force which enhances the distortion in the crystal.

In Figure 5, the lower set of data points may be roughly extrapolated to zero energy at ca. $2.45 < g_{\parallel} < 2.55$, corresponding to degeneracy of the d_{xz}, d_{yz}, and d_{xy} orbitals in a tetrahedral environment. This estimate of $g_{\parallel}$ for $\omega = 90°$ is combined with the ω, $g_{\parallel}$ data points for Cu(P2A-H)$_2$ in toluene (~0°, 2.182), solid Cu(P2A-^{t}Bu)$_2$ (60°, ~2.254), and the bis(2,2′-bipyridylamine)copper(II) ion[24,60] in its perchlorate lattice (56°, 2.244) in Figure 6. The addition of the data (74°, 2.384) for Cs_2CuCl_4 yields an upcurving relationship for $g_{\parallel}$ vs. ω, in which $g_{\parallel}$ increases rapidly with ω as tetrahedral geometry approaches, and this coincides with a prediction based on a crystal field approach.[14] The curve is also well supported by the available data[16,61] for the copper(II) bis chelate of the dimethylbis(3,5-dimethyl-1-pyrazolyl)gallate anion (72°, 2.316). If the $g_{\parallel}$ value of bis(3,3′,5,5′-tetramethyl-4,4′-dicarbethoxydipyrromethenato)copper(II) is approximated by those for which the 4 substituent is –H or –CH$_3$, then the point near (68°, 2.28) may be added as well.[14,62]

The $g_{\parallel}$ and $A_{\parallel}$ values (~2.275, 0.0074 cm^{-1}) for Cu(P2A-^{t}Bu)$_2$ as an impurity in the nonisomorphous Zn(II) lattice cannot reliably be attributed to a regular tetrahedral

Table V. LCAO–MO[a] and ESR[b] Expressions for Pseudotetrahedral D_{2d} Symmetry

$$\phi(\mathrm{b}_2) = \alpha \mathrm{d}_{xy} + \eta \mathrm{p}_z + \rho\phi_\mathrm{L}(xy)$$
$$\phi(\mathrm{e}) = \gamma \mathrm{d}_{xz} + \zeta \mathrm{p}_y + \sigma\phi_\mathrm{L}(xz)$$
$$\phi(\mathrm{e}) = \gamma \mathrm{d}_{yz} + \zeta \mathrm{p}_x + \sigma\phi_\mathrm{L}(yz)$$
$$\phi(\mathrm{b}_1) = \beta \mathrm{d}_{x^2-y^2} + \mu\phi_\mathrm{L}(x^2 - y^2)$$
$$\phi(\mathrm{a}_1) = \delta \mathrm{d}_{3z^2-r^2} + \epsilon \mathrm{s} + \nu\phi_\mathrm{L}(3z^2 - r^2)$$

$$g_\parallel = 2 - \frac{8\alpha\beta\lambda_\mathrm{d}k_{\alpha\beta}}{\Delta_\parallel} \tag{1}$$

$$g_\perp = 2 - \frac{2(\alpha\gamma\lambda_\mathrm{d} - \eta\zeta\lambda_\mathrm{p})(k_{\alpha\gamma} - \eta\zeta)}{\Delta_\perp} \tag{2}$$

$$A_\parallel = \theta + P_\mathrm{d}\left[-\frac{4}{7}\alpha^2 + (g_\parallel - 2)\frac{\alpha\beta}{k_{\alpha\beta}} + \frac{3}{7}(g_\perp - 2)\frac{\alpha\gamma}{k_{\alpha\gamma} - \eta\zeta}\right] + P_\mathrm{p}\left[\frac{4}{5}\eta^2 + \frac{3}{5}(g_\perp - 2)\frac{\eta\zeta}{k_{\alpha\gamma} - \eta\zeta}\right] \tag{3}$$

$$A_\perp = \theta + P_d\left[\frac{2}{7}\alpha^2 + \frac{11}{14}(g_\perp - 2)\frac{\alpha\gamma}{k_{\alpha\gamma} - \eta\zeta}\right] + P_\mathrm{p}\left[-\frac{2}{5}\eta^2 - \frac{13}{10}(g_\perp - 2)\frac{\eta\zeta}{k_{\alpha\gamma} - \eta\zeta}\right] \tag{4}$$

[a] s, p, and ϕ_L represent 4s, 4p, and ligand orbitals, respectively. [b] $k_{\alpha\beta} = \alpha\beta + \beta\rho S_\mathrm{d} + (1 - \beta^2)^{1/2}\rho[T(n)]C/2$; $k_{\alpha\gamma} = \alpha\gamma + \rho\gamma S_\mathrm{d} + (1 - \gamma^2)^{1/2}\rho[T(n)]C/2^{1/2}$; $\theta = -\kappa_0(\alpha^2 P_\mathrm{d} + \eta^2 P_\mathrm{p})$; $P_\mathrm{d,p} = 2\gamma_\mathrm{N}\mu_0 \cdot \mu_\mathrm{N}\langle r^{-3}\rangle_{3\mathrm{d},4\mathrm{p}}$; $\lambda_\mathrm{d,p}$ is the spin–orbit coupling constant for the 3d or 4p orbital of the free copper(II) ion, $S_\mathrm{d,p}$ is the overlap integral of $\langle 3\mathrm{d} \text{ or } 4\mathrm{p}|\phi_\mathrm{L}\rangle$ in the $\phi(\mathrm{b}_2)$ molecular orbital, κ_0 is the Fermi contact term, μ_N and γ_N are the nuclear magneton and gyromagnetic ratio, respectively, C is a geometrical factor which is between 1.00 (planar) and $(2/3)^{1/2}$ (tetrahedral), and $T(n)$ has the same meaning as in the original definition.[65,66] $P_\mathrm{d} = 0.0360$, $P_\mathrm{p} = 0.0402$, $\lambda_\mathrm{d} = -828$ cm^{-1}, and $\lambda_\mathrm{p} = -925$ cm^{-1}.[22] S_d and $T(n)$ are taken to be 0.10 and 0.40, respectively; S_p is assumed for convenience throughout this work to be 0.10. In the limit in which the p-state admixture is negligible ($\eta = \zeta = 0$), the g and A expressions of eq 1–4 take on the customary form for square-planar copper(II) complexes.[66]

structure. Even if the assumption were to be made that the Cu(II) species is distorted to the $\omega = 90°$ supposed for the Zn(II) chelate, the symmetry would be of a tetrahedron elongated[63] toward C_{2v} symmetry.

Little information is available for the d-orbital energies in copper(II) complexes of porphine and its derivatives. This is because there is no obvious procedure for extracting the d–d bands from the broad and intense spectra. A variety of different values has been presumed for the interpretation of ESR results.[64] The significance of Figure 5 is that it is utilizable for a reliable estimation of the d–d band energies of copper porphyrins. In Figure 4, both solid copper(II) tetraphenylporphyrin and its solution are on the lower straight line. The respective band energies, therefore, can be estimated from their $g_\parallel$ values to be ~17 000 and ~20 500 cm^{-1}, using Figure 6.

Theories on the intensity of ligand field absorption bands simply predict that the intensity of d–d transitions increases as the symmetry of the ligand field decreases, since the d–d transitions become allowed as electric dipole transitions.[58] A closer inspection of Table III indicates that the intensities of the Cu(P2A-R)$_2$ complexes initially increase with the bulkiness of R in the first few R groups starting with H but then level off, contrary to the general belief[11,58,59] that the intensity of d–d transitions always continues to increase with the increase in degree of tetrahedral distortion. This seems noteworthy in relation to spectroscopic analyses of copper sites in biological systems.

Bonding Parameters in Pseudotetrahedral Complexes. A hindrance to complete analysis of spectroscopic data in terms of LCAO–MO coefficients and overlap integrals, contact terms, etc. is simply that even with extensive experimental data available, these parameters may be underdetermined.

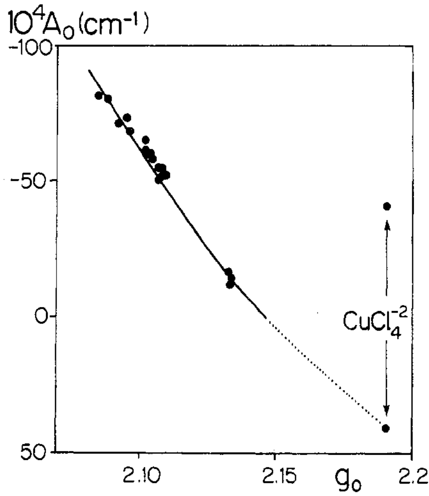

Figure 7. Plot of A_0 against g_0 for pyrrole-2-carboxaldiminates.

Table VI. Computed LCAO–MO Coefficients, κ_0 Values, and Spin–Orbit Coupling Constants Fitted to Observed ESR Data

	$\mathrm{Cs_2CuCl_4}$[a]	Cu(P2A-H)$_2$[b,c]	Cu(P2A-^{t}Bu)$_2$	Cu(TPP)[c,d]
α^2	0.691	0.805	0.805	0.803
β^2	0.745	0.782	0.839	0.783
γ^2	0.691	0.776	0.733	0.517
ρ^2	0.292	0.292	0.250	0.300
η^2	0.078	0	0.020	0
ζ	η	0	η	0
κ_0	0.143	0.380	0.237	0.438

[a] $\eta, \rho < 0$,[18,20] $A_\parallel, A_\perp > 0$, $S_\mathrm{d} = S_\mathrm{p} = 0.1$, $T(n) = 1$, $C = (2/3)^{1/2}$, $\Delta_\parallel = 7730$ cm^{-1}, $\Delta_\perp = 5225$ cm^{-1}, and $\alpha = \gamma$, $\eta = \zeta$, and $\rho = \sigma$ if the symmetry is approximated by T_d. [b] $\Delta_\parallel = 20\,000$ cm^{-1}, $\Delta_\perp = 18\,000$ cm^{-1}. [c] $T(n) = 0.4$, $C = 1.0$, and $\eta = \zeta = 0$ in planar geometry. [d] TPP = *meso*-tetraphenylporphyrin dianion.

In the simple case where the square-planar symmetry of D_{4h} is reduced to D_{2d} by tetrahedral distortion, the one-electron LCAO–MO's of Table V are pertinent, and the expressions for $g_\parallel$, $A_\parallel$, $g_\perp$, and $A_\perp$ which have been obtained via perturbation theory[22] become those of Table V. The ligands are placed between the x and y axes.[21]

Central to the spectral analysis problem is the choice of the value of κ_0, the Fermi contact term for the Cu hyperfine coupling. For archetypal $\mathrm{CuCl_4}^{2-}$, in a definitive paper,[22] the choice of $A_\parallel$ and $A_\perp$ both positive was rejected in favor of the only alternative of $A_\parallel$ and $A_\perp$ both negative, as the latter gave a κ_0 (ca. 0.40) close to the free-ion value (0.43). Of the two points in Figure 7 at $g_0 = 2.191$ for $\mathrm{CuCl_4}^{2-}$, the upper one corresponds to negative A values, whereas the lower one's close relationship to the set of values for the CuN$_4$ systems is suggestive of positive A values as a valid choice, and thus $\kappa_0 < 0.4$. Even without the $\mathrm{CuCl_4}^{2-}$ data, Figure 7 demonstrates that A_0 decreases markedly with g_0 and thus contains the implication that κ_0 decreases below 0.40 as g_0 increases. Indeed, interpretation of the ESR data for the pseudotetrahedral species is difficult, if not impossible, unless this implication is accepted, rather than using $\kappa_0 = 0.40$. Thus, the g and A values of $\mathrm{CuCl_4}^{2-}$ can be fitted with $\kappa_0 = 0.143$ while, for Cu(P2A-H)$_2$, $\kappa_0 = 0.380$ and, for Cu(P2A-^{t}Bu)$_2$, $\kappa_0 = 0.237$ (Table VI) on the condition that increasing the tetrahedral distortion increases α^2, the coefficient which indicates the role of d_{xy} in the b$_2$ orbital. Simultaneously, η^2 increases slightly from 0 to 0.02, corresponding to increased participation of the 4p orbital in the b$_2$ MO. Hence there is a hybridization of

4p with the 3d orbital which is slight but which influences the magnetic properties.

It should be pointed out that the accuracy of the results in Table VI is subject to the uncertainty of the relative orientations of the **g** and **A** tensors.[34]

The tendency for κ_0 to decrease as tetrahedral geometry approaches has been noted previously, and a rationalization was advanced,[15] on the basis of a 3d–4s spin polarization mechanism[67] reducing κ_0.

Copper Porphyrins. Masking of the d–d bands in copper porphyrins by the extremely intense ligand-based transitions has frustrated all experimental approaches[68] to determining d–d band energies and has thus hindered theoretical work on these systems.[64]

Figure 4 suggests that the copper(II) porphyrin systems may be regarded as extreme examples of the CuN_4 chromophores depicted, specifically, as dipyrromethenates with $\omega = 0°$. Hence Figure 5 offers a reliable empirical data base for estimating the crystal field splittings from the ESR parameters. Thus, $g_\parallel = 2.187$, $g_\perp = 2.032$, $A_\parallel = -0.0209\ \mathrm{cm}^{-1}$, and $A_\perp = -0.0032\ \mathrm{cm}^{-1}$ [50] yield estimates of $\Delta_\parallel = 19\,500\ \mathrm{cm}^{-1}$ and $\Delta_\perp = 16\,500\ \mathrm{cm}^{-1}$ for copper(II) tetraphenylporphyrin.

The calculated bonding parameters (Table VI) include a noteworthy value of γ^2 (0.517), which is smaller than often previously estimated[64,66] and which can be considered to indicate strong interaction between the d_{xz}, d_{yz} orbitals and the ligand π system. Guzy et al.[69] have reported similar findings for the phthalocyanine complex. The conclusion[66] that out-of-plane π bonding is negligible is a prejudice with which most ESR data on copper porphyrins have been analyzed, even though it is intuitively acceptable that a fairly strong interaction could exist between the metal d_{xz}, d_{yz} orbitals and the ligand π-electron system. Evidence for this can be often seen in the references.[70,71] Studies on NMR contact shifts, optical absorption spectra, and theoretical calculations for ferric porphyrins also seem to give additional evidence for it.[72]

Redox Potentials. The often interrelated factors which raise the $E°$ of the Cu(II)/Cu(I) couple may be considered to be as follows: (i) those which destabilize the Cu(II) species by reducing its CFSE, either (a) by decreasing ligand σ-donor ability through the use of donor atoms of low donor power or through use of classically electron-withdrawing substituents or (b) by constraining the geometry of the metal center to those of low CFSE, which usually favor copper(I) conversely; (ii) the presence of π-acceptor ("soft") ligands, which favor copper(I).[26]

We are here concerned principally with the effect of geometry on redox potential and, more specifically, with situations where the coordination number is likely to be conserved at 4 for the species involved and only their relative geometries are expected to vary, according to the idealized scheme

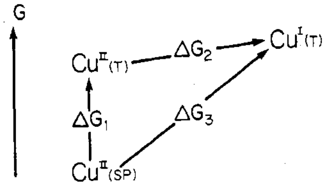

The sign of the apparent free energy change for the redox process depends on the particular half-cell chosen as reference electrode ($\Delta G° = 0$, arbitrarily). Accepting that distortion toward $\omega > 0°$ is a steric constraint on the copper(II) system, which thereby reduces[58] the CFSE the ion would have at $\omega = 0°$, the distortion's consequence is an increase (ΔG_1) in the redox free energy of the copper(II) ion. The copper(I) species, if four-coordinate, would reasonably be expected to be tetrahedral, having the d^{10} configuration. Hence the conversion of a tetrahedral copper(II) species to a tetrahedral copper(I) species is associated with a free energy change (ΔG_2) which is expected to be less than that (ΔG_3) for conversion of a square-planar (but otherwise similar) copper(II) species to the same tetrahedral copper(I) product. The result is that E_2 is less negative than E_3, as borne out by previous data[10] and those below. An alternative viewpoint is to relate the higher redox potential of the tetrahedral species to the decrease in the energy of the partially occupied b_2 orbital, relative to the square-planar situation. A schema of redox potentials vs. $g_\parallel$ for the copper(II) bis(pyrrole-2-carboxaldiminate) chelates, together with some data for bis(salicylaldiminates), is shown in Figure 8. Reference to Table IV confirms that $E_{1/2}$ increases smoothly, indeed almost linearly with $g_\parallel$ for the $Cu(P2A\text{-}Alk)_2$ species, evidencing the degree of tetrahedral distortion as the factor dominating $E_{1/2}$. Correlations of redox potential with spectroscopic properties are known for various types of systems.[73] $Cu(P2A_2\text{-}prn)$ and $Cu(P2A\text{-}R)_2$ molecules with aryl or fluoroalkyl substituents appear to deviate from the otherwise marked correlation. With regard to the latter, these are classically electron-withdrawing groups and as such are expected to destabilize copper(II) relative to copper(I) at given geometry. Related to this is the observation that the difference in $E_{1/2}$ values between bis(*N*,*N'*-R_2-β-diketiminato)copper(II) compounds with R = CH_3 and R = Ph is also larger[10] (0.7 V) than is attributable solely to a geometric factor, and a conjugative interaction with the aryl group could be invoked. Obviously the cooperation of several factors can lead to large $E_{1/2}$ changes.

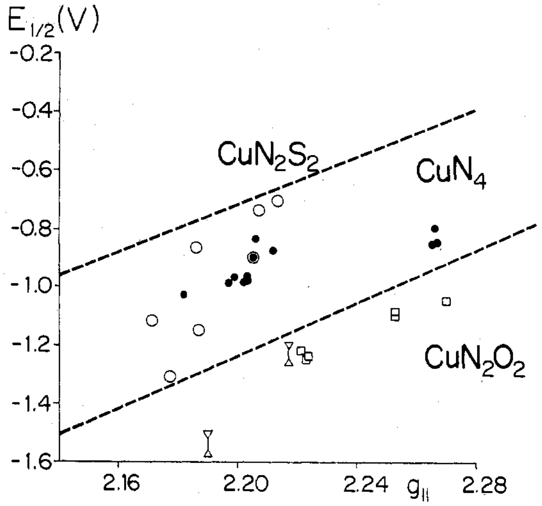

Figure 8. Schema of redox potential vs. $g_\parallel$ for copper(II) chelates: $Cu(P2A\text{-}Alk)_2$ (●), other pyrrole-2-carboxaldiminates (○), and salicylaldiminates from this work (□) and ref 10 (△, ▽).

Nonetheless, it is clear from Figure 8 that the CuN_4 species distribute themselves along a diagonal region which is paralleled by an $E_{1/2}$:$g_\parallel$ domain for related CuN_2O_2 centers, shifted down by a few hundred millivolts. CuN_2S_2 species must occupy a parallel region about 300 mV above the CuN_4 domain, on the basis of the known data.[10] Extension of the CuN_4 domain to $\omega = 75°$ would suggest that, ceteris paribus, conversion from square to flattened tetrahedral geometry increases the $E_{1/2}$ by ca. 0.5 V.

Blue Copper Centers in Proteins. These intensely absorbing (600–650 nm) species have high redox potentials and small hyperfine interactions ($|A_\perp|$, $|A_\parallel| < 0.007\ \mathrm{cm}^{-1}$). Planar macrocyclic tetrathiaether complexes of copper(II) have similar absorption and redox properties,[8] but there is as yet no evidence that their ESR behavior resembles that of the blue copper proteins. Low-temperature absorption, CD and MCD,[9] and XPS[12] studies are consistent with flattened tetrahedral N_3S coordination about the Cu(II).

Peisach and Blumberg[74] have shown that for a four-coordinate copper(II) system of constant donor atom set, e.g., CuN_4, $|A_{\parallel}|$ decreases and $g_{\parallel}$ increases as the total formal positive charge on these five atoms increases. Our results demonstrate that at constant charge, the same type of relationship arises via tetrahedral distortion. We have used the $g_{\parallel}$ and $|A_{\parallel}|$ values (2.10 and 0.0185 cm^{-1}, respectively[75]) for the planar molecule *N,N′*-ethylenebis(monothioacetylacetoniminato)copper(II) as a base point in Figure 4 for defining a $A_{\parallel}$ vs. $g_{\parallel}$ region for the CuN_2S_2 chromophore. If this species' $A_{\parallel}:g_{\parallel}$ relationship as a function of angle of twist toward regular tetrahedral geometry can be represented as parallel to the CuN_4 and CuN_2O_2 systems, then the relationship for CuN_3S centers may be taken as the mean of those for CuN_2S_2 and CuN_4[76] for neutral molecules. The dashed lines shown in Figure 4 define, at low $A_{\parallel}$, a region in which the $A_{\parallel}:g_{\parallel}$ data for a number of blue copper proteins appear.

Inferences drawn from Figures 4–6 should be applicable to many Cu(II) systems with peptide nitrogen as ligand, as the $g_{\parallel}$ and $|A_{\parallel}|$ values (2.160, 0.022 cm^{-1} [77]) of the planar[78] CuN_4 moiety in $[Cu(glyglyglygly)]^{2-}$ fall on the correlation line in Figure 4.

In addition, assignment of the 600-nm region band to a CT absorption[8,79] is supported by our observation that ϵ reaches a limiting value at low ω.

$E^{\circ\prime}$ values associated with planar copper(II) sites (e.g., +0.42 V[80] in nonblue superoxide dismutase, with the planar[2] $Cu(imidazole)_4$ moiety) can be raised by 0.2 V by a tetrahedral distortion of only $\omega = 60°$ (Figure 6).

We conclude that the spectroscopic and redox properties of these pseudotetrahedral CuN_4 systems, combined with information for essentially planar CuN_2S_2 systems, form a data base which supports the assignment of pseudotetrahedral geometry and the presence of sulfur donor(s) in the copper binding site of "blue" proteins.

Acknowledgment. This work is a contribution from the Bioinorganic Chemistry Group, supported by Operating and Negotiated Development Grants from the National Research Council of Canada. The authors express their appreciation to Dr. T. Takui for his valuable suggestions on metal porphyrins and to Drs. G. R. Brubaker and F. G. Herring for their interest in this work.

Registry No. $Cu(P2A\text{-}H)_2$, 16389-89-2; $Cu(P2A\text{-}Me)_2$, 15170-37-3; $Cu(P2A\text{-}Et)_2$, 15170-38-4; $Cu(P2A\text{-}Tfe)_2$, 62006-87-5; $Cu(P2A\text{-}n\text{-}Pr)_2$, 62057-42-5; $Cu(P2A\text{-}i\text{-}Pr)_2$, 15170-39-5; $Cu(P2A\text{-}n\text{-}Bu)_2$, 15153-57-8; $Cu(P2A\text{-}i\text{-}Bu)_2$, 62006-88-6; $Cu(P2A\text{-}s\text{-}Bu)_2$, 62057-43-6; $Cu(P2A\text{-}c\text{-}Hx)_2$, 26430-77-3; $Cu(P2A\text{-}Norb)_2$, 62006-89-7; $Cu(P2A\text{-}Dpm)_2$, 62006-90-0; $Cu(P2A\text{-}Dma)_2$, 62006-91-1; $Cu(P2A\text{-}t\text{-}Bu)_2$, 38626-58-3; $Cu(P2A\text{-}Adam)_2$, 62029-60-1; $Cu(P2A\text{-}Dmpe)_2$, 62006-92-2; $Cu(P2A_2\text{-}en)$, 21297-41-6; $Cu(P2A_2\text{-}prn)$, 21297-44-9; $Cu(P2A_2\text{-}bun)$, 21297-45-0; Cs_2CuCl_4, 13820-31-0; Cu(TPP), 14172-91-9.

References and Notes

(1) On leave from Tohoku University, Sendai, Japan.
(2) J. S. Richardson, K. A. Thomas, B. H. Rubin, and D. C. Richardson, *Proc. Natl. Acad. Sci. U.S.A.*, **72**, 1349 (1975).
(3) O. Siiman, N. M. Young, and P. R. Carey, *J. Am. Chem. Soc.*, **98**, 744 (1976).
(4) A. J. M. S. Uiterkamp, H. van der Deen, H. C. J. Berendsen, and J. F. Boas, *Biochim. Biophys. Acta*, **372**, 407 (1974).
(5) L. E. Bennett, *Prog. Inorg. Chem.*, **18**, 1 (1973).
(6) (a) J. A. Fee, *Struct. Bonding (Berlin)*, **23**, 1 (1975), and references therein; (b) T. Vänngård in "Biological Applications of Electron Spin Resonance", H. M. Swartz, J. R. Bolton, and D. C. Borg, Ed., Wiley-Interscience, New York, N.Y., 1972.
(7) M. D. Glick, D. P. Gavel, L. L. Diaddario, and D. B. Rorabacher, *Inorg. Chem.*, **15**, 1190 (1976).
(8) T. E. Jones, D. B. Rorabacher, and L. A. Ochrymowycz, *J. Am. Chem. Soc.*, **97**, 7485 (1975).
(9) E. I. Solomon, J. W. Hare, and H. B. Gray, *Proc. Natl. Acad. Sci. U.S.A.*, **71**, 1389 (1976).
(10) G. S. Patterson and R. H. Holm, *Bioinorg. Chem.*, **4**, 257 (1975).
(11) A. S. Brill and G. F. Bryce, *J. Chem. Phys.*, **48**, 4398 (1968).
(12) E. I. Solomon, P. J. Clendening, H. B. Gray, and F. J. Grunthaner, *J. Am. Chem. Soc.*, **97**, 3878 (1975).
(13) Y. Murakami, Y. Matsuda, and K. Sakata, *Inorg. Chem.*, **10**, 1728 (1971).
(14) Y. Murakami, Y. Matsuda, and K. Sakata, *Inorg. Chem.*, **10**, 1734 (1971).
(15) H. Yokoi, *Bull. Chem. Soc. Jpn.*, **47**, 3037 (1974).
(16) Dmpz = 3,5-dimethylpyrazolyl. F. G. Herring, D. J. Patmore, and A. Storr, *J. Chem. Soc., Dalton Trans.*, 711 (1975).
(17) R. C. Rosenberg, C. A. Root, P. K. Bernstein, and H. B. Gray, *J. Am. Chem. Soc.*, **97**, 2092 (1975).
(18) L. L. Lohr and W. N. Lipscomb, *Inorg. Chem.*, **2**, 911 (1963).
(19) J. Ferguson, *J. Chem. Phys.*, **40**, 3406 (1964).
(20) D. W. Smith, *J. Chem. Soc. A*, 2900 (1970).
(21) C. A. Bates, W. S. Moore, K. J. Standley, and K. W. H. Stevens, *Proc. Phys. Soc., London*, **79**, 73 (1962).
(22) M. Sharnoff, *J. Chem. Phys.*, **42**, 3383 (1965).
(23) G. F. Kokoszka, C. W. Reimann, and H. C. Allen, Jr., *J. Phys. Chem.*, **71**, 121 (1967).
(24) B. J. Dudley, B. J. Hathaway, and P. G. Hodgson, *J. Chem. Soc., Dalton Trans.*, 882 (1972).
(25) J. Ferguson, *J. Chem. Phys.*, **35**, 1612 (1961).
(26) B. R. James and R. J. P. Williams, *J. Chem. Soc.*, 2007 (1961).
(27) C. J. Hawkins and D. D. Perrin, *J. Chem. Soc.*, 1351 (1962); 2996 (1963).
(28) K. Yeh and R. H. Barker, *Inorg. Chem.*, **6**, 830 (1967).
(29) R. H. Holm, A. Chakravorty, and L. J. Theriot, *Inorg. Chem.*, **5**, 625 (1966).
(30) A. Chakravorty and T. S. Kannan, *J. Inorg. Nucl. Chem.*, **29**, 1691 (1967).
(31) G. E. Batley and D. P. Graddon, *Aust. J. Chem.*, **21**, 1473 (1968).
(32) C. M. Harris and E. Sinn, *J. Inorg. Nucl. Chem.*, **30**, 2723 (1968).
(33) J. H. Weber, *Inorg. Chem.*, **6**, 258 (1967).
(34) K. Shibata, "Methods of Biochemical Analysis", Vol. 7, D. Glick, Ed., Interscience, New York, N.Y., 1959, p 77; *ibid.*, Vol. 9, 1962, p 217.
(35) We are grateful to a referee for reminding us of this possibility.
(36) T. Vänngård and R. Aasa, *Paramagn. Reson., Proc. Int. Conf., 1st, 1962*, 509 (1963).
(37) A. D. Toy, S. H. H. Chaston, J. R. Pilbrow, and T. D. Smith, *Inorg. Chem.*, **10**, 2219 (1971).
(38) H. Yokoi and T. Isobe, *Bull. Chem. Soc. Jpn.*, **42**, 2187 (1969).
(39) F. G. Herring and R. L. Tapping, *Can. J. Chem.*, **52**, 4016 (1974), and references therein.
(40) H. Yokoi, unpublished work.
(41) R. Wilson and D. Kivelson, *J. Chem. Phys.*, **44**, 4445 (1966).
(42) D. P. Graddon, *J. Inorg. Nucl. Chem.*, **14**, 161 (1960).
(43) R. L. Belford, M. Calvin, and G. Belford, *J. Chem. Phys.*, **26**, 1165 (1957).
(44) R. H. Wopschall and I. Shain, *Anal. Chem.*, **39**, 1514 (1967).
(45) R. S. Nicholson and I. Shain, *Anal. Chem.*, **36**, 706 (1964).
(46) Apart from any liquid junction potential correction. See ref 10.
(47) D. H. Busch, *Helv. Chim. Acta*, Werner Commemorative Edition, 191 (1967).
(48) R. Tewari and R. G. Srivastava, *Acta Crystallogr., Sect. B*, **27**, 1644 (1971).
(49) C. H. Wei, *Inorg. Chem.*, **11**, 2315 (1972).
(50) P. T. Manaharan and M. T. Rogers, "Electron Spin Resonance of Metal Complexes", T. F. Yen, Ed., Plenum Press, New York, N.Y., 1969, p 143.
(51) H. Yokoi and T. Kishi, *Chem. Lett.*, 749 (1973).
(52) J. I. Zink and R. S. Drago, *J. Am. Chem. Soc.*, **94**, 4550 (1972).
(53) H. Yokoi, M. Sai, and T. Isobe, *Bull. Chem. Soc. Jpn.*, **43**, 1078 (1970).
(54) B. R. McGarvey, *J. Phys. Chem.*, **71**, 51 (1967).
(55) L. Helmholz and R. F. Kruh, *J. Am. Chem. Soc.*, **74**, 1176 (1952).
(56) R. G. Pearson, *J. Am. Chem. Soc.*, **85**, 3533 (1963); *Science*, **151**, 172 (1966).
(57) E. Sinn and C. M. Harris, *Coord. Chem. Rev.*, **4**, 391 (1969).
(58) C. J. Ballhausen, "Introduction to Ligand Field Theory", McGraw-Hill New York, N.Y., 1962, pp 108, 185.
(59) D. W. Smith, *Struct. Bonding (Berlin)*, **12**, 49 (1972), and references therein.
(60) J. E. Johnson, T. A. Beinecke, and R. A. Jacobson, *J. Chem. Soc. A*, 2124 (1971).
(61) D. J. Patmore, D. F. Rendle, A. Storr, and J. Trotter, *J. Chem. Soc., Dalton Trans.*, 718 (1975).
(62) M. Elder and B. R. Penfold, *J. Chem. Soc. A*, 2556 (1969).
(63) C. H. Wei, *Inorg. Chem.*, **11**, 1100 (1972).
(64) P. W. Lau and W. C. Lin, *J. Inorg. Nucl. Chem.*, **37**, 2389 (1975).
(65) A. H. Maki and B. R. McGarvey, *J. Chem. Phys.*, **29**, 31 (1958).
(66) D. Kivelson and R. Neiman, *J. Chem. Phys.*, **35**, 149 (1961).
(67) A. J. Freeman and R. E. Watson, *Magnetism*, **2A**, 167 (1965).
(68) J. J. Leonard and F. R. Longo, *J. Am. Chem. Soc.*, **95**, 8506 (1973); *J. Phys. Chem.*, **79**, 62 (1975).
(69) C. M. Guzy, J. B. Raynor, and M. C. R. Symons, *J. Chem. Soc. A*, 2299 (1969).
(70) A. D. Adler, Ed., *Ann. N.Y. Acad. Sci.*, **206** (1973); **244** (1975).
(71) D. W. Clack and M. S. Farrimond, *J. Chem. Soc., Dalton Trans.*, **29** (1972).
(72) (a) G. N. La Mar, G. R. Eaton, R. H. Holm, and F. A. Walker, *J. Am. Chem. Soc.*, **95**, 63 (1973); (b) G. N. La Mar and F. A. Walker, *ibid.*, **95**, 1782 (1973); (c) H. Kobayashi, Y. Yanagawa, H. Osada, S. Minami, and M. Shimizu, *Bull. Chem. Soc. Jpn.*, **46**, 1471 (1973).

(73) A. A. Vlček, *Electrochim. Acta*, **13**, 1063 (1968).
(74) J. Peisach and W. E. Blumberg, *Arch. Biochem. Biophys.*, **165**, 691 (1974).
(75) R. S. Giordano and R. D. Bereman, *Inorg. Nucl. Chem. Lett.*, **10**, 203 (1974).
(76) H. Yokoi, M. Otagiri, and T. Isobe, *Bull. Chem. Soc. Jpn.*, **44**, 2395 (1971).
(77) K. E. Falk, H. C. Freeman, T. Jansson, B. G. Malmström, and T. Vänngård, *J. Am. Chem. Soc.*, **89**, 6071 (1967).
(78) H. C. Freeman and M. R. Taylor, *Acta Crystallogr.*, **18**, 939 (1965).
(79) D. R. McMillin, R. C. Rosenberg, and H. B. Gray, *Proc. Natl. Acad. Sci. U.S.A.*, **71**, 4760 (1974).
(80) J. A. Fee and P. E. di Corleto, *Biochemistry*, **12**, 4893 (1973).

Contribution from the Laboratory of Analytical Chemistry,
Faculty of Science, Nagoya University, Nagoya 464, Japan

Reactions of Hydrogen Peroxide with Metal Complexes. 2. Kinetic Studies on the Peroxo Complex Formation of Nitrilotriacetatodioxovanadate(V) and Dioxo(2,6-pyridinedicarboxylato)vanadate(V)

SHIGENOBU FUNAHASHI, KENSAKU HARAGUCHI,[1] and MOTOHARU TANAKA*

Received November 4, 1976 AIC60797C

The kinetics of the reactions of hydrogen peroxide with nitrilotriacetatodioxovanadate(V) (V^VNTA, $VO_2(nta)^{2-}$) and dioxo(2,6-pyridinedicarboxylato)vanadate(V) (V^VPDA, $VO_2(pda)(H_2O)^-$) have been studied spectrophotometrically using a stopped-flow technique at an ionic strength of 1.0 mol dm^{-3} ($NaClO_4$) in the pH range 1.5–5 between 15 and 35 °C. The rate of the peroxo complex formation of V^VNTA is expressed as $d[VO(O_2)(nta)^{2-}]/dt = (k_1 + k_2[H^+])[VO_2(nta)^{2-}][H_2O_2]$ where $k_1 = 7.41$ $mol^{-1}\ dm^3\ s^{-1}$ ($\Delta H^{\ddagger} = 39 \pm 1$ kJ mol^{-1}, $\Delta S^{\ddagger} = -96 \pm 9$ J K^{-1} mol^{-1}) and $k_2 = 1.86 \times 10^4$ $mol^{-2}\ dm^6\ s^{-1}$ ($\Delta H^{\ddagger} = 39 \pm 1$ kJ mol^{-1}, $\Delta S^{\ddagger} = -33 \pm 9$ J K^{-1} mol^{-1}). The rate of the peroxo complex formation of V^VPDA is as follows: $d[VO(O_2)(pda)(H_2O)^-]/dt = \{k_1[H^+][VO_2(pda)(H_2O)^-] + k_2[VO_2(pda)(H_2O)^-] + k_3[VO_2(pda)(OH)^{2-}]\}[H_2O_2]$ where $k_1 = 4.1 \times 10^2$ $mol^{-2}\ dm^6\ s^{-1}$ ($\Delta H^{\ddagger} = 24 \pm 1.5$ kJ mol^{-1}, $\Delta S^{\ddagger} = -114 \pm 9$ J K^{-1} mol^{-1}), $k_2 = 0.39$ $mol^{-1}\ dm^3\ s^{-1}$ ($\Delta H^{\ddagger} = 46 \pm 2$ kJ mol^{-1}, $\Delta S^{\ddagger} = -97 \pm 9$ J K^{-1} mol^{-1}), and $k_3 = 28$ $mol^{-1}\ dm^3\ s^{-1}$ ($\Delta H^{\ddagger} = 35 \pm 2$ kJ mol^{-1}, $\Delta S^{\ddagger} = -100 \pm 9$ J K^{-1} mol^{-1}). Mechanisms are proposed for the H_2O_2 insertion reaction and in terms of activation parameters some discussions are made on the difference in the reactivities of these complexes. We have studied the protonation equilibria of PDA where $\log K_1 = 4.62 \pm 0.02$ ($\Delta H_1 = -27 \pm 4$ kJ mol^{-1}, $\Delta S_1 = -2 \pm 10$ J K^{-1} mol^{-1}), $\log K_2 = 2.18 \pm 0.02$, and $\log K_3 = 0.49 \pm 0.02$, the complexation equilibrium of the V^V–PDA complex where $[VO_2(pda)(H_2O)^-]/[VO_2^+][pda^{2-}] = 10^{8.65\pm0.10}$, and the hydrolysis of the V^V–PDA complex where $[VO_2(pda)(OH)^{2-}][H^+]/[VO_2(pda)(H_2O)^-] = 10^{-5.87\pm0.02}$ ($\Delta H = 7 \pm 7$ kJ mol^{-1}, $\Delta S = -78 \pm 20$ J K^{-1} mol^{-1}).

Introduction

Reactions of hydrogen peroxide with various chemical species have been extensively studied.[2,3] From the chemical point of view, the redox reaction of H_2O_2 has been the subject matter of many investigations. Especially because of its biochemical significance, there has been a good deal of interest in kinetic studies on formation, decomposition, and substrate reactions of peroxo compounds of biologically important metal complexes such as catalase and peroxidase.[4-8] However, relatively little attention has been drawn to the processes of coordination of hydrogen peroxide to metal complexes preceding the decompositions of hydrogen peroxide.[9,10] There is increasing evidence that vanadium has a significant biological role,[11,12] although it has been established to be an essential element only for a few organisms.[13,14]

The kinetics of formation of the pentavalent vanadium complex has been little investigated. Recently the kinetics of formation of vanadium(V) complexes with aminopolycarboxylate ions have been reported.[15] Since some data are available on the kinetics of vanadium(V) reactions, we attempt to compare the water-exchange rate with hydrogen peroxide insertion rates for vanadium(V).

The purpose of the present work is to examine differences in the reactivities of some vanadium(V) complexes for peroxo complex formation,[16] to determine the energetics of the reaction, and to provide new information on the reaction mechanism. In this paper we describe the results on the reactions

$$V^VNTA + H_2O_2 \rightleftharpoons V^V(NTA)H_2O_2 \qquad (1)$$

$$V^VPDA + H_2O_2 \rightleftharpoons V^V(PDA)H_2O_2 \qquad (2)$$

where NTA and PDA refer to nitrilotriacetic acid (H_3nta) and 2,6-pyridinedicarboxylic acid (H_2pda).

As the data on the equilibrium between vanadium(V) ion and 2,6-pyridinedicarboxylic acid were not available, we have studied the protonation equilibria of PDA and the complexation equilibria of the V^V–PDA complex. We have also determined the thermodynamic parameters for hydrolysis of the V^V–PDA complex which are necessary to analyze kinetic results.

Experimental Section

Reagents. Sodium Perchlorate. Reagent grade sodium perchlorate was prepared by neutralizing 60% perchloric acid with reagent grade anhydrous sodium carbonate. Heavy-metal impurities in the sodium perchlorate solution were precipitated together with active carbon as hydroxides at pH 8.5. After evaporation of the solution crystals of sodium perchlorate were obtained by cooling the solution. Sodium perchlorate was then crystallized twice from distilled water.

Sodium Hydroxide. Sodium hydroxide solution was prepared by electrolysis of the solution of pure sodium perchlorate obtained as described above.

Hydrogen Peroxide. A 60% hydrogen peroxide solution without added stabilizers (Mitsubishi Edogawa Kagaku Co., Japan) was purified by distillation under reduced pressure. A solution of hydrogen peroxide was titrated with a standard permanganate.

Vanadium(V) Perchlorate. Reagent grade ammonium metavanadate was recrystallized twice from purified ammonia water. Pure ammonium metavanadate was dissolved in sodium hydroxide solution and transformed to vanadate ion. Ammonia was expelled by bubbling the solution with nitrogen gas. Vanadium(V) perchlorate solution (ca. 10^{-2} mol dm^{-3}) was prepared by addition of perchloric acid. Vanadium(V) was reduced by sulfur dioxide and the resulting vanadium(IV) was standardized titrimetrically against a standard potassium permanganate.